Fermilab FERMILAB-Conf-01/332-E E791 Nov. 2001

Light Meson Physics from Charm Decays at Fermilab E791

Carla Göbel [1]

Instituto de Física, Facultad de Ingeniería, Universidad de la República, C.C. 30, CP 11300, Montevideo, Uruguay

Abstract. We present recent results on light mesons based on Dalitz plot analyses of charm decays from Fermilab experiment E791. Scalar mesons are found to have large contributions to the decays studied, $D^+ \to K^-\pi^+\pi^+$ and $D^+, D_s^+ \to \pi^-\pi^+\pi^+$. From the $K\pi\pi$ final state, we find good evidence for the existence of the light and broad κ meson and we measure its mass and width. We also discuss recently published results on the 3π final states, especially the measurement of the f_0 parameters and the evidence for the σ meson from $D^+ \to \sigma\pi^+$. These results demonstrate the importance of charm decays as a new environment for the study of light meson physics.

INTRODUCTION

The decays of charm mesons are currently a new source of information for the study of light meson spectroscopy, with the advantages of having well defined initial state (the D meson, a 0^- state with defined mass). This new information is complementary to that from scattering experiments and can be particularly relevant to the understanding of the scalar sector.

Here we present preliminary results for the Dalitz-plot analysis of the Cabibbo-favored decay $D^+ \to K^-\pi^+\pi^+$ using data from Fermilab E791 experiment. We also present an overview of our results for $D_s^+ \to \pi^-\pi^+\pi^+$ [1] and $D^+ \to \pi^-\pi^+\pi^+$ [2] Dalitz-plot analyses. The E791 data was collected in 1991/92 from 500 GeV/c π^--nucleon interactions. For details see [3].

For the $D^+ \to K^-\pi^+\pi^+$ analysis, when we include all known $K\pi$ resonant channels plus a non-resonant (NR) contribution, we find that the NR decay is dominant. This is unusual in D decays. Moreover, the fit model has important discrepancies with respect to the data. By including an extra scalar resonant state, with unconstrained mass and width, we obtain a fit which is substantially superior to that without this state. The values for its mass and width are found to be $797 \pm 19 \pm 42$ MeV/c^2 and $410 \pm 43 \pm 85$ MeV/c^2 respectively. We refer to this state as the κ. The existence of such a state has been greatly discussed in the literature in recent years [4]–[14]. We also obtain new measurements for the mass and the width of the $K_0^*(1430)$ resonance: $1459 \pm 7 \pm 6$ MeV/c^2 and $175 \pm 12 \pm 12$ MeV/c^2 respectively.

From our analysis of $D_s^+ \to \pi^-\pi^+\pi^+$ decays, we find that the dominant decay fraction

[1] For the E791 Collaboration.

comes from $f_0(980)\pi^+$. We obtain new measurements for the $f_0(980)$ and $f_0(1370)$ masses and widths. From $D^+ \to \pi^-\pi^+\pi^+$ decays, we find that a model with only known $\pi\pi$ resonances plus a NR channel is not able to describe the data adequately. We find strong evidence for the presence of a light and broad scalar resonance, the $\sigma(500)$, the $\sigma\pi^+$ channel being responsible for half of the decay rate. We measure the mass and the width of this scalar meson to be $478^{+24}_{-23} \pm 17$ MeV/c^2 and $324^{+42}_{-40} \pm 21$ MeV/c^2, respectively.

THE $D^+ \to K^-\pi^+\pi^+$ DALITZ-PLOT ANALYSIS

From the original 2×10^9 events collected by E791, and after reconstruction and selection criteria, we obtained the $D^+ \to K^-\pi^+\pi^+$ sample shown in Figure 1(a). The filled area represents the level of background; besides the combinatorial, the other main source of background comes from the reflection of the decay $D_s^+ \to K^-K^+\pi^+$ (through $\bar{K}^*K^+$ and $\phi\pi^+$). The crosshatched region contains the events selected for the Dalitz-plot analysis. There are 15090 events in this sample, of which 6% are background.

Figure 1(b) shows the Dalitz-plot for these events. The two axes are the squared invariant-mass combinations for $K\pi$, and the plot is symmetrized with respect to the two identical pions. The plot presents a rich structure, where we can observe the clear bands from $\bar{K}^*(890)\pi^+$, and an accumulation of events at the upper edge of the diagonal, due to heavier resonances. To study the resonant substructure, we perform an unbinned maximun-likelihood fit to the data, with probability distribution funtions (PDF's) for both signal and background sources. In particular, for each candidate event, the signal PDF is written as the square of the total physical amplitude A (defined below) and it is weighted for the acceptance across the Dalitz plot (obtained by Monte Carlo (MC)) and by the level of signal to background for each event, as given by the line shape of Figure 1(a). The background PDF's (levels and shapes) are fixed for the Dalitz-plot fit, according to MC and data studies.

We begin describing our first approach to fit the data, which represents the conventional Dalitz-plot analysis including the known $K\pi$ resonant amplitudes ($A_n,\ n \geq 1$), plus a constant non-resonant contribution. The signal amplitude is constructed as a coherent sum of the various sub-channels:

$$A = a_0 e^{i\delta_0} A_0 + \sum_{n=1}^{N} a_n e^{i\delta_n} A_n(m_{12}^2, m_{13}^2) \tag{1}$$

Each resonant amplitude is written as

$$A_n = BW_n\, F_D^{(J)}\, F_n^{(J)}\, M_n^{(J)}\ . \tag{2}$$

where BW_n is the relativistic Breit-Wigner propagator

$$BW_n = \frac{1}{m_0^2 - m^2 - i m_0 \Gamma(m)} \tag{3}$$

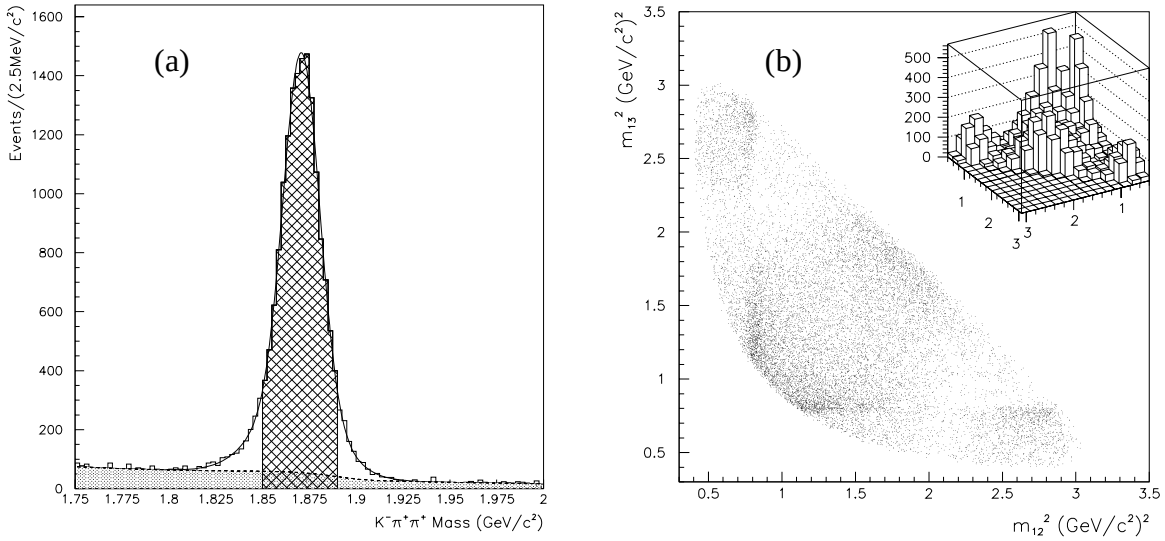

FIGURE 1. (a) The $K^-\pi^+\pi^+$ invariant mass spectrum. The filled area is background; (b) Dalitz plot corresponding to the events in the dashed area of (a).

with mass dependent width,

$$\Gamma(m) = \Gamma_0 \frac{m_0}{m} \left(\frac{p^*}{p_0^*} \right)^{2J+1} \left(\frac{F_n^{(J)}(p^*)}{F_n^{(J)}(p_0^*)} \right)^2 . \tag{4}$$

The quantities F_D and F_R are the Blatt-Weisskopf damping factors respectively for the D and the $K\pi$ resonances, they depend on the radii of the decaying meson and are set to $r_D = 3.0$ GeV^{-1} and $r_R = 1.5$ GeV^{-1} [18]; p^* is the pion momentum in the resonance rest frame at mass m_{12} ($p_0^* = p^*(m_0)$). $M_n^{(J)}$ describes the angular distribution due to the spin J of the resonance. See details in [2]. Finally each amplitude is Bose symmetrized $A_n = A_n[(\mathbf{12})\mathbf{3}] + A_n[(\mathbf{13})\mathbf{2}]$.

Using this model (Model A), we find contributions from the following channels: the non-resonant, responsible for more than 90% of the decay rate, followed by $\bar{K}_0^*(1430)\pi^+$, $\bar{K}^*(892)\pi^+$, $\bar{K}^*(1680)\pi^+$ and $\bar{K}_2^*(1430)\pi^+$. The decay fractions and relative phases are shown in Table 1. These values are in accordance with previous results from E691 [15] and E687 [16]. We thus confirm a high non-resonant contribution according to this model, which is totally unusual in D decays. Besides, there is an important destructive interference pattern, since all fractions add up to 140 %.

To evaluate the fit quality of Model A, we compute a two-dimensional χ^2 in the Dalitz plot, from the difference in densities for the model (from a fast-MC algorithm) and the data. We obtain $\chi^2/\nu = 2.7$ (ν being the number of degrees of freedom), with a corresponding confidence level (CL) of 10^{-11}. In Figure 2(a) we show the $K\pi$ low and high squared-mass projections for data (error bars) and model (solid line). The discrepancies are evident at the very low-mass region for $m^2(K\pi)_{low}$ and near

TABLE 1. Results without κ (Model A) and with κ (Model B). *Preliminary*.

Decay Mode	Model A: No κ Fraction (%)	Phase	Model B: With κ Fraction (%)	Phase
NR	90.9 ± 2.6	0° (fixed)	$13.0 \pm 5.8 \pm 2.6$	$(349 \pm 14 \pm 8)°$
$\kappa\pi^+$	–	–	$47.8 \pm 12.1 \pm 3.7$	$(187 \pm 8 \pm 17)°$
$\bar{K}^*(892)\pi^+$	13.8 ± 0.5	$(54 \pm 2)°$	$12.3 \pm 1.0 \pm 0.9$	0° (fixed)
$\bar{K}_0^*(1430)\pi^+$	30.6 ± 1.6	$(54 \pm 2)°$	$12.5 \pm 1.4 \pm 0.4$	$(48 \pm 7 \pm 10)°$
$\bar{K}_2^*(1430)\pi^+$	0.4 ± 0.1	$(33 \pm 8)°$	$0.5 \pm 0.1 \pm 0.2$	$(306 \pm 8 \pm 6)°$
$\bar{K}^*(1680)\pi^+$	3.2 ± 0.3	$(66 \pm 3)°$	$2.5 \pm 0.7 \pm 0.2$	$(28 \pm 13 \pm 15)°$

2.5 $(\text{GeV/c}^2)^2$ for $m^2(K\pi)_{high}$. These regions of disagreement are the same observed previously by E687 [16]. We thus conclude that a model with the known $K\pi$ resonances, plus a non-resonant amplitude, is not able to describe the $D^+ \to K^-\pi^+\pi^+$ Dalitz plot satisfactorily.

A similar pattern – bad fit quality with large NR fraction – is found in the analysis of the decay $D^+ \to \pi^-\pi^+\pi^+$ when allowing only the established $\pi\pi$ resonances [2] . There we find that the inclusion of an extra scalar resonance improves the fit substantially, giving strong evidence for the $\sigma(500)$. See the section on $D^+ \to \pi^-\pi^+\pi^+$ below. Thus, we are lead to try an extra scalar resonance in our fit model here. The possible existence of a light and broad $K\pi$ scalar state has been suggested by many authors [4, 5, 6, 7, 8], some of them believing it would be a member of a light scalar nonet [9, 10, 11]; however, its existence has been the subject of some controversy also[12, 13, 14].

A second fit model, Model B, is constructed by the inclusion of an extra scalar state, with unconstrained mass and width. For consistency, the mass and width of the other scalar state, the $K_0^*(1430)$, are also free parameters of the fit. We adopt a better description for these scalar states by introducing gaussian-type form-factors [12] to take into account the finite size of the decaying mesons. Two extra floating parameters are the meson radii r_D and r_R introduced above.

Using this model, we obtain the values of $797 \pm 19 \pm 42$ MeV/c^2 for the mass and $410 \pm 43 \pm 85$ MeV/c^2 for the width of the new scalar state (first error statistical, second error systematic), referred to here as the κ. The values of mass and width obtained for the $K_0^*(1430)$ are respectively $1459 \pm 7 \pm 6$ MeV/c^2 and $175 \pm 12 \pm 12$ MeV/c^2, appearing heavier and narrower than presented by the PDG [17]. The decay fractions and relative phases for Model B, with systematic errors, are given in Table 1. Compared to the results of Model A (without κ), the non-resonant mode drops from over 90% to 13%. The $\kappa\pi^+$ state is now the dominant channel with about 50%. The meson radii r_D and r_R are found to be respectively 5.0 ± 0.5 GeV^{-1} and 1.6 ± 1.3 GeV^{-1}, in complete agreement with previous estimates [18, 19].

Moreover, the fit quality of Model B is substantially superior to that of Model A. The χ^2/ν is now 0.73 with a CL of 95%. The very good agreement between the model and the data can be seen in the projections of Figure 2(b).

A number of studies were done to check these results. For example, we replaced the complex κ Breit-Wigner by a real Breit-Wigner, with no phase variation. In this case, we got similar mass and width for this extra state, but with unphysical fractions for this state and the NR, and a worse fit quality. We also replaced the κ by a hypothetical

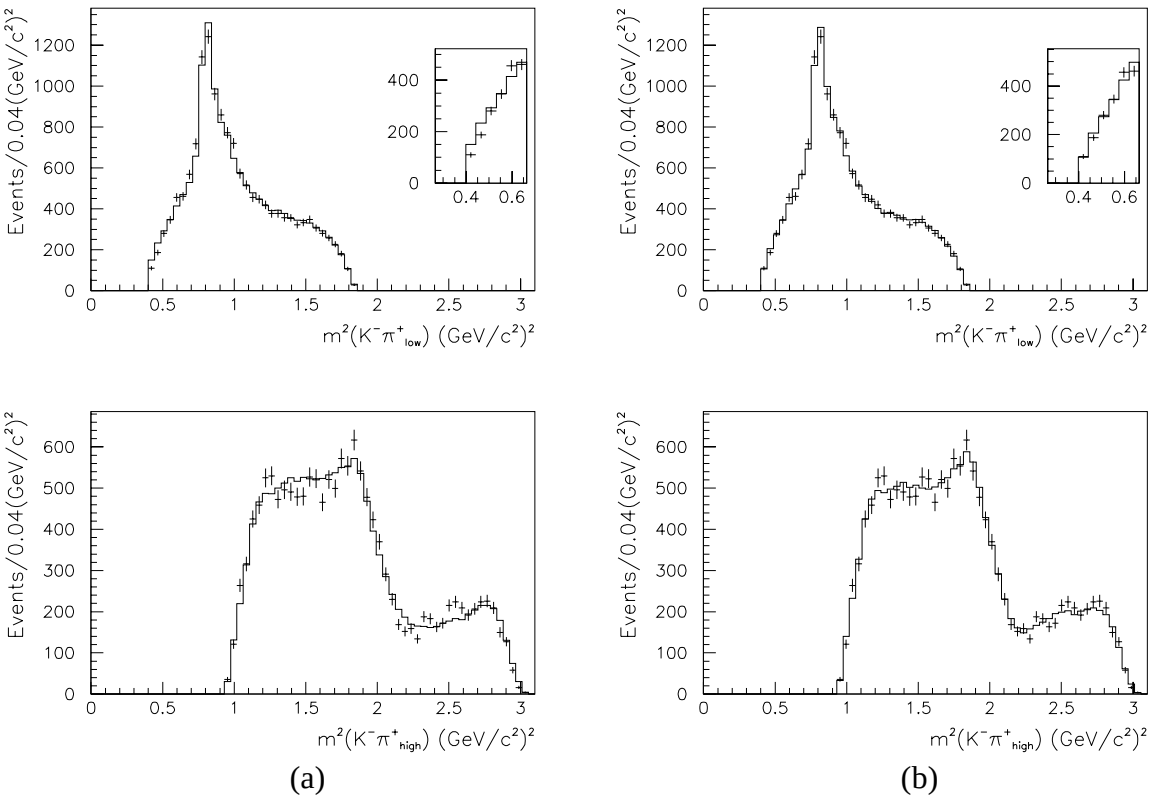

FIGURE 2. $m^2(K\pi_{\rm low})$ and $m^2(K\pi_{\rm high})$ projections for data (error bars) and fast MC (solid line): (a) fit to Model A, without κ, and (b) fit to Model B, with κ.

vector state, with unconstrained mass and width, but it appears with a small fraction, the fit quality being comparable to the model without it, and all fractions and phases remaining unchanged. A tensor model was also tried without convergence, the width being driven to large, negative values. Other models with the κ were also tried. For example, modifications to the scalar Breit-Wigner amplitude and to the form-factors were introduced. A number of studies for the parameterization of the NR amplitude were tried [22], with and without the κ. No model without the κ was able to describe our data satisfactorily. All variations of models with κ gave similar results for the κ mass and width (within errors) although the fractions for κπ and NR showed correlations.

Thus, from the results above, we find strong evidence that a light and broad scalar $K\pi$ resonance gives an important contribution to the $D^+ \to K^-\pi^+\pi^+$ decay.

THE $D_S^+ \to \pi^-\pi^+\pi^+$ RESULTS

In Figure 3 we show the $\pi^-\pi^+\pi^+$ invariant mass distribution for the sample collected by E791 after reconstruction and selection criteria [1, 2]. Besides combinatorial background, reflections from the decays $D^+ \to K^-\pi^+\pi^+$, $D^+ \to K^-\pi^+$ (plus one extra

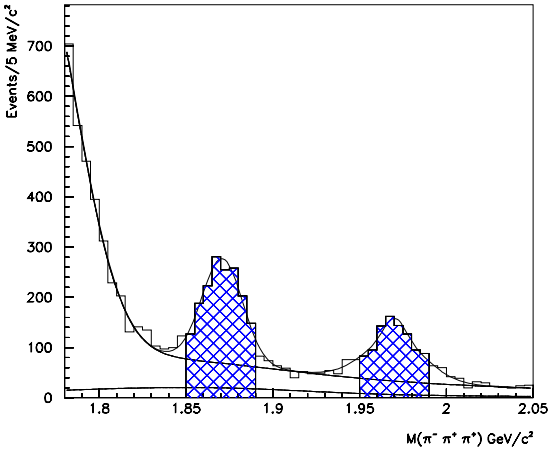

FIGURE 3. The $\pi^-\pi^+\pi^+$ invariant mass spectrum. The dotted line represents the $D^0 \to K^-\pi^+$ plus $D_s^+ \to \eta'\pi^+$ reflections and the dashed line is the total background. Events used for the Dalitz analyses are in the hatched areas.

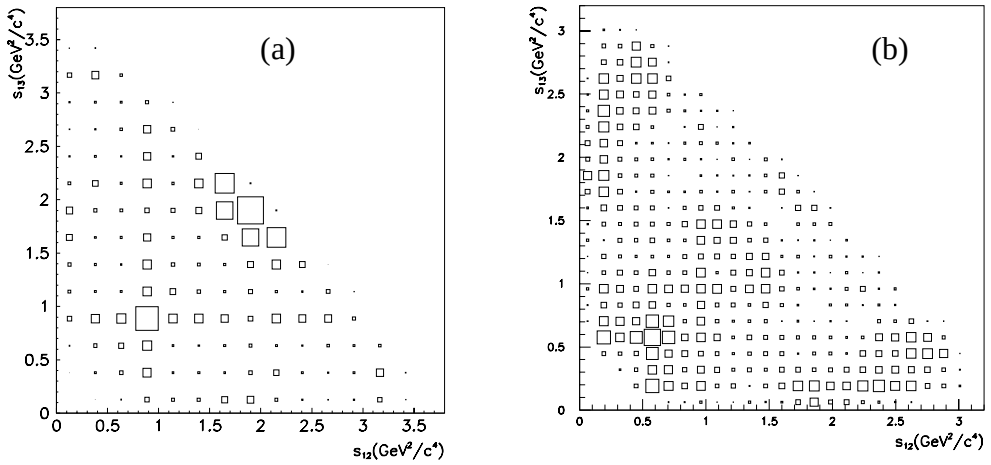

FIGURE 4. (a) The $D_s^+ \to \pi^-\pi^+\pi^+$ Dalitz plot and (b) the $D^+ \to \pi^-\pi^+\pi^+$ Dalitz plot. Since there are two identical pions, the plots are symmetrized.

track) and $D_s^+ \to \eta'\pi^+$, $\eta' \to \rho^0(770)\gamma$ are all taken into account. The hatched regions in Figure 3 show the samples used for the Dalitz-plot analyses. There are 1686 and 937 candidate events for D^+ and D_s^+ respectively, with a signal to background ratio of about 2:1. The Dalitz plots for these events are shown in Figure 4, the axes corresponding to the two $\pi^-\pi^+$ invariant-masses squared. For the Dalitz-plot fits of both $D^+ \to \pi^-\pi^+\pi^+$ and $D_s^+ \to \pi^-\pi^+\pi^+$ decays, we use essentially the same formalism as for the $D^+ \to K^-\pi^+\pi^+$ decays. See details in [1, 2].

TABLE 2. Dalitz fit results for $D_s^+ \to \pi^-\pi^+\pi^+$.

Decay Mode	Fraction (%)	Phase
$f_0(980)\pi^+$	$56.5 \pm 4.3 \pm 4.7$	0° (fixed)
NR	$0.5 \pm 1.4 \pm 1.7$	$(181 \pm 94 \pm 51)^\circ$
$\rho^0(770)\pi^+$	$5.8 \pm 2.3 \pm 3.7$	$(109 \pm 24 \pm 5)^\circ$
$f_2(1270)\pi^+$	$19.7 \pm 3.3 \pm 0.6$	$(133 \pm 13 \pm 28)^\circ$
$f_0(1370)\pi^+$	$32.4 \pm 7.7 \pm 1.9$	$(198 \pm 19 \pm 27)^\circ$
$\rho^0(1450)\pi^+$	$4.4 \pm 2.1 \pm 0.2$	$(162 \pm 26 \pm 17)^\circ$

For the $D_s^+ \to \pi^-\pi^+\pi^+$ events in Figure 4(a), the signal amplitude includes the following channels: $\rho^0(770)\pi^+$, $f_0(980)\pi^+$, $f_2(1270)\pi^+$, $f_0(1370)\pi^+$, $\rho^0(1450)\pi^+$ and the non-resonant, assumed constant across the Dalitz plot.

For the $f_0(980)\pi^+$ amplitude, instead of a simple Breit-Wigner of Eq. 3 [2], we use a coupled-channel Breit-Wigner function [23],

$$BW_{f_0(980)} = \frac{1}{m_{\pi\pi}^2 - m_0^2 + i m_0(\Gamma_\pi + \Gamma_K)} , \tag{5}$$

$$\Gamma_\pi = g_\pi \sqrt{m_{\pi\pi}^2/4 - m_\pi^2},\ \Gamma_K = \frac{g_K}{2}\left(\sqrt{m_{\pi\pi}^2/4 - m_{K^+}^2} + \sqrt{m_{\pi\pi}^2/4 - m_{K^0}^2} \right). \tag{6}$$

The $D_s^+ \to \pi^-\pi^+\pi^+$ Dalitz plot is fit to obtain not only the decay fractions and phases of the possible sub-channels, but also the parameters of the $f_0(980)$ state, g_π, g_K, and m_0, as well as the mass and width of the $f_0(1370)$. The other resonance masses and widths are taken from the PDG[17]. The resulting fractions and phases are given in Table 2.

The measured $f_0(980)$ parameters are $m_0 = 977 \pm 3 \pm 2$ MeV/c^2, $g_\pi = 0.09 \pm 0.01 \pm 0.01$ and $g_K = 0.02 \pm 0.04 \pm 0.03$. Our value for g_π is in very good agreement with OPAL and MARKII results [24], but WA76 [23] found a much larger value, $g_\pi = 0.28 \pm 0.04$. Our value of g_K indicates a small coupling of $f_0(980)$ to $K\bar{K}$. The values of the $f_0(980)$ mass and of g_π, as well as the magnitudes and phases of the resonant amplitudes, are relatively insensitive to the value of g_K. Both OPAL and MARKII results are also insensitive to the value of g_K. WA76, on the contrary, measured $g_K = 0.56 \pm 0.18$.

By fitting the Dalitz plot using for the $f_0(980)$ a simple Breit-Wigner function, we find $m_0 = 975 \pm 3$ MeV/c^2 and $\Gamma_0 = 44 \pm 2 \pm 2$ MeV/c^2, and the results for fractions and phases are indistinguishable.

The confidence level of the fit for $D_s^+ \to \pi^-\pi^+\pi^+$ is 35% [1]. In Figure 5 we show the $\pi^-\pi^+$ mass-squared projections for data (points) and model (solid lines, from fast-MC).

As we can see by the results of Table 2, approximately half of the $D_s^+ \to \pi^-\pi^+\pi^+$ rate is via $f_0(980)\pi^+$. If the spectator amplitude is dominant in this decay, this would support the interpretation of the $f_0(980)$ as an $s\bar{s}$ state. On the other hand, the large contribution from $f_0(1370)\pi^+$ indicates the presence of either W-annihilation amplitudes or strong rescattering in the final state. In fact, the $f_0(1370)\pi^+$ is not observed in the $D_s^+ \to$

[2] For both $D, D_s \to 3\pi$ analyses, the relativistic Breit-Wigner for each resonant amplitude is defined with a factor (-1) with respect to Eq. 3.

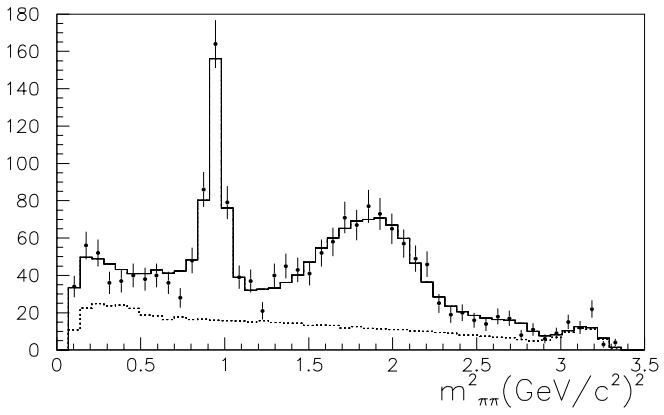

FIGURE 5. s_{12} and s_{13} ($m^2_{\pi\pi}$) projections for $D_s^+ \to \pi^-\pi^+\pi^+$ data (dots) and our best fit (solid). The hashed area corresponds to background.

$K^+K^-\pi^+$ final state[25], pointing to the $f_0(1370)$ being a non-$s\bar{s}$ state, as suggested by the naive quark model[17]. There is no evidence in the D_s^+ decay for a low-mass broad scalar particle as seen in the $D^+ \to \pi^-\pi^+\pi^+$ decay, discussed below.

THE $D^+ \to \pi^-\pi^+\pi^+$ DECAY

In a first approach, we try to fit the $D^+ \to \pi^-\pi^+\pi^+$ Dalitz plot of Figure 4(b) with the same amplitudes used for the $D_s^+ \to \pi^-\pi^+\pi^+$ analysis. Using this model, the non-resonant, the $\rho^0(1450)\pi^+$, and the $\rho^0(770)\pi^+$ amplitudes are found to dominate, as shown in Table 3, and in agreement with previous reported analyses [26, 27]. However, this model does not describe the data satisfactorily, especially at low $\pi^-\pi^+$ mass squared, as can be seen from Fig. 6(a). The χ^2/ν obtained from the binned Dalitz plot for this model is 1.6, with a CL less than 10^{-5}.

To investigate the possibility that another $\pi^-\pi^+$ resonance contributes to the $D^+ \to \pi^-\pi^+\pi^+$ decay, we add an extra scalar resonance amplitude to the signal PDF, with mass and width as floating parameters in the fit.

We find that this model improves our fit substantially. The mass and the width of the extra scalar state are found to be $478^{+24}_{-23} \pm 17$ MeV/c^2 and $324^{+42}_{-40} \pm 21$ MeV/c^2, respectively. Refering to this state as the σ, we obtain that the $\sigma\pi^+$ chanell produces the largest decay fraction, as shown in Table 3; the non-resonant amplitude, which is dominant in the model without $\sigma\pi^+$, drops substantially. This model describes the data much better, as can be seen by the $\pi\pi$ mass squared projection in Fig. 6(b). The χ^2/ν is now 0.9, with a corresponding confidence level of 91%.

The existence of a light $\pi\pi$ state, or the σ, has been the subject of a long-standing controversy [28, 29]. Various experiments have presented inconsistent evidence for this state [30], yielding conflicting results [17, 29].

TABLE 3. Dalitz fit results for $D^+ \to \pi^-\pi^+\pi^+$. First errors are statistical, second systematics (only for fit with $\sigma\pi^+$ mode).

Decay Mode	Fit without $\sigma\pi^+$		Fit with $\sigma\pi^+$	
	Fraction (%)	Phase	Fraction (%)	Phase
$\sigma\pi^+$	–	–	$46.3 \pm 9.0 \pm 2.1$	$(206 \pm 8 \pm 5)^\circ$
$\rho^0(770)\pi^+$	20.8 ± 2.4	0° (fixed)	$33.6 \pm 3.2 \pm 2.2$	0° (fixed)
NR	38.6 ± 9.7	$(150 \pm 12)^\circ$	$7.8 \pm 6.0 \pm 2.7$	$(57 \pm 20 \pm 6)^\circ$
$f_0(980)\pi^+$	7.4 ± 1.4	$(152 \pm 16)^\circ$	$6.2 \pm 1.3 \pm 0.4$	$(165 \pm 11 \pm 3)^\circ$
$f_2(1270)\pi^+$	6.3 ± 1.9	$(103 \pm 16)^\circ$	$19.4 \pm 2.5 \pm 0.4$	$(57 \pm 8 \pm 3)^\circ$
$f_0(1370)\pi^+$	10.7 ± 3.1	$(143 \pm 10)^\circ$	$2.3 \pm 1.5 \pm 0.8$	$(105 \pm 18 \pm 1)^\circ$
$\rho^0(1450)\pi^+$	22.6 ± 3.7	$(46 \pm 15)^\circ$	$0.7 \pm 0.7 \pm 0.3$	$(319 \pm 39 \pm 11)^\circ$

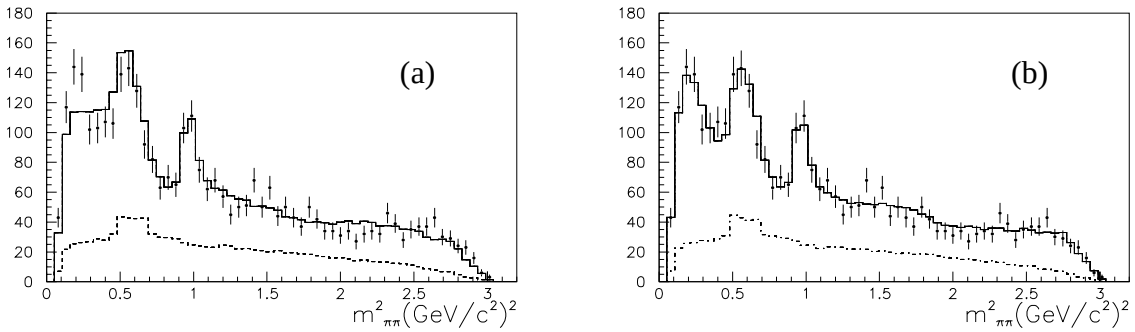

FIGURE 6. s_{12} and s_{13} ($m^2_{\pi\pi}$) projections for $D^+ \to \pi^-\pi^+\pi^+$ data (dots) and our best fit (solid) for models (a) without and (b) with $\sigma\pi^+$ amplitude. The dashed distribution corresponds to the expected background level.

To test the model above, we replace the scalar amplitude by vector and tensor states, and also by a real Breit-Wigner, with no phase variation (as also done in the $D^+ \to K^-\pi^+\pi^+$ analysis). All these alternative models fail to describe the data as well as the scalar (regular) Breit-Wigner amplitude. See detailed discussion in [2].

CONCLUSION

From the data of the Fermilab E791 experiment, we studied the Dalitz plots of the decays $D^+ \to K^-\pi^+\pi^+$, $D_s^+ \to \pi^-\pi^+\pi^+$ and $D^+ \to \pi^-\pi^+\pi^+$. In these three final states, the scalar intermediate resonances were found to give the main contribution to the decay rates. We obtained strong evidence for the existence of the σ and κ scalar mesons, measuring their masses and widths. We also obtained new measurements for masses and widths of the other scalars studied, $f_0(980)$, $f_0(1430)$ and $K_0^*(1430)$.

The results presented here show the potential of D meson decays for the study of light meson espectroscopy, in particular in the scalar sector.

REFERENCES

1. E791 Collaboration, E.M. Aitala *et al.*, Phys. Rev. Lett. **86** 765 (2001).
2. E791 Collaboration, E.M. Aitala *et al.*, Phys. Rev. Lett. **86** 770 (2001).
3. J.A. Appel, Ann. Rev. Nucl. Part. Sci. **42**, 367 (1992); D. Summers *et al.*, hep-ex/0009015; S. Amato *et al.*, Nucl. Instr. Meth. A **324**, 535 (1993); E791 Collaboration, E.M. Aitala *et al.*, Eur. Phys. J. direct C **4**, 1 (1999).
4. E. van Beveren *et al.*, Z. Phys. C **30**, 615 (1986).
5. S. Ishida *et al.*, Prog. Theor. Phys. **98**, 621 (1997).
6. D. Black *et al.*, Phys. Rev. D **58**, 054012 (1998).
7. J.A. Oller, E. Oset, J.R. Peláez, Phys. Rev. D **59** 074001 (1999); M. Jamin, J.A. Oller, and A. Pich, Nucl. Phys. **B587**, 331 (2000).
8. C.M. Shakin, H. Wang, Phys. Rev. D **63**, 014019 (2001).
9. M. Ishida, Prog. Theor. Phys. **101**, 661 (1999).
10. D. Black *et al.*, Phys. Rev. D **59**, 074026 (1999).
11. J.A. Oller and E. Oset, Phys. Rev. D **60**, 074023 (1999).
12. N.A. Törnqvist, Z. Phys. C **68**, 647 (1995).
13. A.V. Anisovitch and A.V. Sarantsev, Phys. Lett. B **413**, 137 (1997).
14. S.N. Cherry and M.R. Pennington, Nucl. Phys. **A688** 823 (2001).
15. E691 Collaboration, J.C. Anjos *et al.*, Phys. Rev. D **48**, 56 (1993).
16. E687 Collaboration, P.L. Frabetti *et al.*, Phys. Lett. B **331**, 217 (1994).
17. Particle Data Group, D.E. Groom *et al.*, Eur. Phys. Jour. C **15**, 1 (2000).
18. ARGUS Collaboration, H. Albrecht *et al.*, Phys. Lett. B **308**, 435(1993).
19. CLEO Collaboration, S. Kopp *et al.*, Phys. Rev. D **63**, 092001 (2001).
20. J.M. Blatt and V.F. Weisskopf, Theoretical Nuclear Physics, John Wiley & Sons, New York, 1952.
21. LASS Collaboration, D. Aston *et al.*, Nucl. Phys. **B296**, 493 (1988).
22. I. Bediaga, C. Göbel, and R. Méndez-Galain, Phys. Rev. Lett. **78**, 22 (1997) and Phys. Rev. D **56**, 4268 (1997); C. Göbel, Ph.D. Thesis, Centro Brasileiro de Pesquisas Físicas, Rio de Janeiro, Brazil (1999).
23. WA76 Collaboration, T.A. Armstrong *et al.*, Z. Phys. C **51**, 351 (1991).
24. OPAL Collaboration, K. Ackerstaff *et al.*, Eur. Phys. J. C **4**, 19 (1998); MARKII Collaboration, G. Gidal *et al.*, Phys. Lett. B **107**, 153 (1981).
25. E687 Collaboration, P.L. Frabetti *et al.*, Phys. Lett. B **351**, 591 (1995).
26. E691 Collaboration, J.C. Anjos *et al.*, Phys. Rev. Lett. **62**, 125 (1989).
27. E687 Collaboration, P.L. Frabetti *et al.*, Phys. Lett. B **407**, 79 (1997).
28. M.R. Pennington, in *Proceedings of the Workshop on Hadron Spectroscopy*, Frascati Physics Series Vol. XV (Laboratory Nazionali de Frascati, Frascati (Roma), Italy, 1999), p. 95.
29. N. Törnqvist, in *Proceedings of the Workshop on Hadron Spectroscopy*, Frascati Physics Series Vol. XV (Laboratory Nazionali de Frascati, Frascati (Roma), Italy, 1999), p. 237, and N. Törnqvist, hep-ph/0008135.
30. WA102 Collaboration, D. Barberis *et al.*, Phys. Lett. B **453**, 316 (1999); CLEO Collaboration, D.M. Asner *et al.*, Phys. Rev. D **61**, 012002 (2000); GAMS Collaboration, D. Alde *et al.*, Phys. Lett. B **397** , 350 (1997).